AGU PUBLICATIONS

Water Resources Research

RESEARCH ARTICLE
10.1002/2015WR018054

Improvement of the hillslope-storage Boussinesq model by considering lateral flow in the unsaturated zone

Jun Kong[1,2], Chengji Shen[2,3], Zhaoyang Luo[2], Guofen Hua[2], and Hongjun Zhao[2]

[1]Jiangsu Key Laboratory of Coast Ocean Resources Development and Environment Security, Hohai University, Nanjing, China, [2]State Key Laboratory of Hydrology-Water Resources and Hydraulic Engineering, Hohai University, Nanjing, China, [3]National Centre for Groundwater Research and Training, School of Civil Engineering, University of Queensland, Brisbane, Queensland, Australia

Key Points:
- Unsaturated lateral flow plays an important role in the hillslope drainage process
- Lateral flow in the unsaturated zone is considered in the HSB model
- An equivalent propagation thickness in the vadose zone is analytically expressed

Supporting Information:
- Supporting Information S1

Correspondence to:
J. Kong,
kongjun999@126.com

Citation:
Kong, J., C. Shen, Z. Luo, G. Hua, and H. Zhao (2016), Improvement of the hillslope-storage Boussinesq model by considering lateral flow in the unsaturated zone, *Water Resour. Res.*, *52*, 2965–2984, doi:10.1002/2015WR018054.

Received 1 SEP 2015
Accepted 23 MAR 2016
Accepted article online 28 MAR 2016
Published online 17 APR 2016

Abstract Unsaturated flow is an important factor that affects groundwater motion. Among various drainage models, the nonlinear Hillslope-storage Boussinesq (HSB) model has been commonly used to predict water flux along a slope. In this study, we improved this model by considering lateral flow in the unsaturated zone. Using modified van Genuchten functions, we analytically expressed the concept of equivalent propagation thickness in the vadose zone. This analytical expression was then incorporated into the HSB model to reflect two different stages of the drainage process and to simulate the hillslope drainage process more accurately. The model results indicated that lateral flow has significant effects in the unsaturated zone during the hillslope drainage process. Even in sandy aquifers, the amount of water contributed by the unsaturated zone is a key factor that enables a decrease in the water table during the middle and late stages of the process. A comparison between the measured and simulated results based on both convergent-type and divergent-type hillslope drainage processes revealed that the thickness of the saturated zone decreases as the unsaturated flow increases. This study emphasizes the necessity of considering unsaturated flow in the HSB model to improve the accuracy of predicting groundwater outflow rates and develop more accurate hydrographs. The concept of equivalent propagation thickness also provides a criterion for assessing the importance of unsaturated lateral flow for future drainage research.

1. Introduction

Hydraulic groundwater theory has been widely applied in investigations of various problems in catchment hydrology, of which hillslope drainage is a critical process that has received increasing attention over the past several years [*Troch et al*., 2013]. The outlet of a hillslope is where runoff forms, and the outflow rate strongly determines the interaction intensity between subsurface and surface flows in river channels. Therefore, understanding the hillslope drainage process can help identify the runoff components and control subsurface contaminants discharging into surface water [*Dahl et al*., 2007].

To study the hillslope drainage process, 2-D/3-D numerical models based on variable-saturation equations (e.g., Richards' equation) have been used, but these models require large computational resources, even for small-scale problems, and their parameterization is difficult due to uncertainties associated with the subsurface properties [*Bresciani et al*., 2014]. Given these problems, researchers began to investigate the Boussinesq-type equations, which are more computationally efficient and robust. By incorporating a width function along the length of a hillslope into the traditional Boussinesq equation, *Troch et al*. [2003] developed the Hillslope-storage Boussinesq (HSB) model to more efficiently simulate the subsurface flow in a sloping, unconfined aquifer. The efficiency of the HSB model primarily lies in its one-dimensional (1-D) form and its simplicity of being analytically solved for different problems [*Serrano*, 1995; *Troch et al*., 2002; *Rocha et al*., 2007] based on the Dupuit assumption [*Bresciani et al*., 2014]. In particular, it allows for a better understanding of the hillslope storage drainage process by resetting the source/sink term within the model [*Brutsaert*, 1994; *Verhoest and Troch*, 2000; *Troch et al*., 2004; *Hogarth et al*., 2014].

In the HSB model, drainable porosity is an important parameter that affects the prediction accuracy. In the original HSB model [*Troch et al*., 2003], constant drainable porosity was introduced and defined as the ratio of drained water content to the change in water elevation [*Bear*, 1972]. In practice, drainable porosity

changes spatially and temporally, as during the drainage process; additionally, the extents of the saturated and unsaturated zones decrease and increase, respectively. Considering this, it is more physically meaningful to treat drainable porosity as a transient value; *Neuman* [1987] defined it as the released water content per unit area per unit decline of the water table. Based on *Neuman*'s [1987] definition, capillarity should indirectly influence drainable porosity; this has also been confirmed by certain experimental studies [*Parlange and Brutsaert*, 1987; *Fink et al*., 2001; *Nachabe*, 2002; *Phi et al*., 2013]. Using the Brooks-Corey parameterization for the unsaturated zone, *Nachabe* [2002] derived the relationship between the drainable porosity and water table elevation at different drainage stages. More recently, by modifying the *van Genuchten* [1980] function, *Hilberts et al*. [2005] derived an analytical expression related to the water table elevation and applied it to the original HSB model. The simulation results of their revised model exhibited better accuracy than the original HSB model. However, these HSB models were based on either constant or alterable drainable porosity and thus underestimated the hydrographs measured in laboratory experiments, particularly during the late stage of the drainage process. The discrepancy between the simulated and measured values indicates that certain other mechanisms should be considered in an accurate HSB model. Traditional HSB models emphasize water movement in the saturated zone and neglects the effect of the vadose zone, which has been found to alter water movement in the saturated zone and thus groundwater table fluctuations [*Cartwright et al*., 2005; *Moench*, 2008; *Cardenas*, 2010]. The assumption of negligible effects of the vadose zone is valid only when the scale of the unsaturated zone is significantly small [*Gillham*, 1984] or under the steady state flow condition [*Romano et al*., 1999]. *Barry et al*. [1996] noted that without considering the vadose zone, the calculation of groundwater change and water storage in an unconfined aquifer could be substantially inaccurate. The vadose zone can store or release water and thus alter groundwater table fluctuations [*Paniconi et al*., 2003]. In coastal beaches, unsaturated horizontal flow can promote groundwater wave propagation [*Kong et al*., 2013, 2015]. For inland highway drainage engineering, saturated flow models that neglect unsaturated flow will tend to overpredict the groundwater table elevation [*Dan et al*., 2012, 2013]. The importance of the vadose zone was considered by *Hilberts et al*. [2007], who further improved the HSB model by coupling it with a 1-D Richards' equation to account for vertical flow in the unsaturated zone. Their model somewhat resolves the problem of delay between recharge and outflow but still fails to completely overcome this discrepancy because the coupled model of *Hilberts et al*. [2007] assumes unsaturated flow to be vertical and neglects the lateral component, which might play an important role in the hillslope drainage process.

Inspired by the work of *Hilberts et al*. [2005], this study aims to further improve the HSB model by considering unsaturated lateral flow during the drainage process. This paper is organized as follows: in section 2, we describe the derivation of the improved HSB model by considering lateral flow in the unsaturated zone. In section 3, the new HSB model is verified against previous HSB models using both numerical results based on Richards' equation and experimental results. In section 4, the features and influence of unsaturated flow during the drainage are discussed, and conclusions are drawn in section 5.

2. Derivation of the Improved HSB Model

As shown in Figure 1, following the mass balance principle, the governing equation for the HSB model can be expressed as [*Troch et al*., 2003]:

$$\frac{\partial S}{\partial t} = -\frac{\partial wq}{\partial x} + Nw \tag{1}$$

where S [L^2] is the total available water storage per unit distance along the hillslope; the x axis is parallel to the sloping bed; w [L] is the hillslope width that changes along the slope; q [$L^2\ T^{-1}$] is the Darcy flux per unit width along the hillslope; N [$L\ T^{-1}$] is the groundwater recharge rate due to precipitations and is set equal to zero when only the drainage process is considered.

The total available storage normal to the hillslope can be calculated as:

$$S = w\int_0^D (\theta - \theta_r)\mathrm{d}z \tag{2}$$

where D [L] is the aquifer thickness normal to the impermeable hillslope base; θ and θ_r are the soil water content and residual water content, respectively.

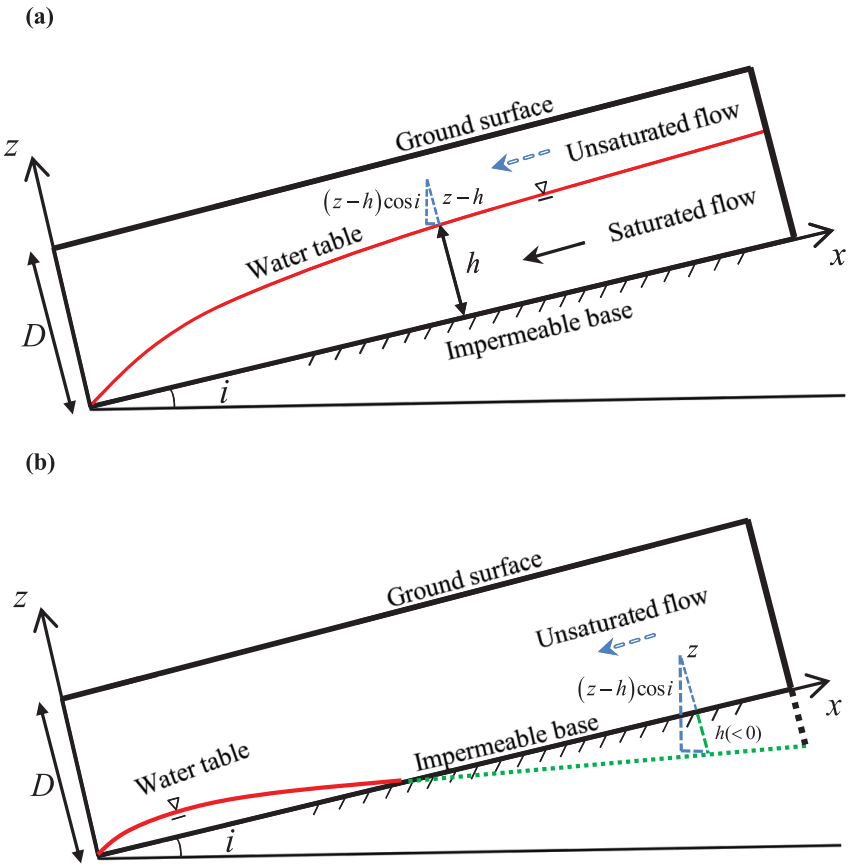

Figure 1. Schematic diagram of a sloping unconfined aquifer with slope angle *i*. (a) The early and middle saturated and unsaturated drainage stages; (b) the late unsaturated drainage stage.

Instead of using the assumption of *Hilberts et al*. [2005], we assumed that the pressure distribution along the direction normal to the hillslope base is hydrostatic. Under this assumption, the hydraulic gradient in the unsaturated zone is equal to that in the saturated zone along a hillslope, and the flow direction is parallel to the base. Therefore, the total flux per unit width along a hillslope can be expressed as the sum of fluxes per unit width in saturated and unsaturated zones (Figure 1a):

$$\begin{aligned} wq = w(q_s + q_{us}) &= -w\frac{\partial \Phi}{\partial x}\left(\int_0^h K_s \mathrm{d}z + \int_h^D K(\psi)\mathrm{d}z\right) \\ &= -w\frac{\partial \Phi}{\partial x}\left(K_s h + \int_h^D K(\psi)\mathrm{d}z\right) \\ \text{with}\ \frac{\partial \Phi}{\partial x} &= \frac{\partial h}{\partial x}\cos i + \sin i \end{aligned} \tag{3a}$$

where h [L] is the water table elevation along the direction normal to the sloping bed; i is the slope; q_s [$L^2\ T^{-1}$] and q_{us} [$L^2\ T^{-1}$] are the fluxes per unit width along the hillslope in the saturated and unsaturated zones, respectively; Φ [L] is the piezometric head and $\Phi = z + \psi$, where z is the elevation [L] and ψ is the pressure head [L] (positive in the saturated zone and negative in the unsaturated zone); and K_s [$L\ T^{-1}$] and $K(\psi)$ [$L\ T^{-1}$] are the hydraulic conductivities of the saturated and unsaturated zones, respectively.

However, it should be noted that equation (3a) is applicable only when the saturated and unsaturated zones coexist (i.e., the unsaturated zone is located above the saturated zone during the early and middle drainage stages) along the direction normal to the hillslope (Figure 1a). In fact, such a coexistence does not last throughout the whole drainage process. Instead, in the late stage, a fully unsaturated zone begins to develop from the upstream part of the hillslope (right side of Figure 1b), where only unsaturated flow

facilitates the drainage, due to the decline of the water table. As the water table falls, the absolute value of the negative pressure in the fully unsaturated zone increases, leading to a redistribution of the pore water. Consequently, certain amount of the pore water in the fully unsaturated zone flows downslope. The flux per unit width in the fully unsaturated zone can be expressed as:

$$wq = wq_{us} = -w\frac{\partial \Phi}{\partial x}\int_0^D K(\psi)\mathrm{d}z \tag{3b}$$

In the unsaturated zone, under the homogeneity assumption, the hydraulic conductivity $K(\psi)$ and soil moisture $\theta(\psi)$ are both related to the pressure head ψ; this relationship can be described by the *van Genuchten* [1980] functions:

$$\begin{cases} \theta = \theta_r + (\theta_s - \theta_r)S_W \\ K(\psi) = K_s S_W^{1/2}\left[1-\left(1-S_W^{1/m}\right)^m\right]^2 \end{cases} \tag{4a}$$

where:

$$S_W = \left[\frac{1}{1+(\alpha_{VG}\psi)^n}\right]^m \tag{4b}$$

$$m = 1 - 1/n \tag{4c}$$

where α_{VG} [L^{-1}] and n are the van Genuchten parameters related to soil properties; θ_s is the saturated water content; S_W is the effective saturation and has a value between 0 and 1; and $\psi = (h-z)\cos i$ under the hydrostatic pressure assumption along the direction normal to hillslope base (Figure 1).

It is difficult to derive the analytical solution of equation (2) by directly substituting in equation (4). Given the complexity of the van Genuchten functions, *Troch* [1993] found that by assuming $m = 1 + 1/n_1$ ($n_1 \neq n$), it is possible to fit the soil moisture retention curves for a variety of soil types:

$$\theta = \theta_r + (\theta_s - \theta_r)\left[\frac{1}{1+(\alpha\psi)^{n_1}}\right]^{(1+1/n_1)} \tag{5}$$

where α [L^{-1}] and n_1 are new parameters. Based on this modification, by substituting equation (5) into equation (2), we can obtain the following expression when $h \geq 0$ (early and middle stages):

$$\begin{aligned} S &= w\int_0^D (\theta(\psi)-\theta_r)\mathrm{d}z = w\left[\int_0^h (\theta_s-\theta_r)\mathrm{d}z + \int_h^D (\theta(\psi)-\theta_r)\mathrm{d}z\right] \\ &= w(\theta_s-\theta_r)h + w\int_h^D (\theta_s-\theta_r)\{1+[\alpha(h-z)\cos i]^{n_1}\}^{(-1-1/n_1)}\mathrm{d}z \\ &= w(\theta_s-\theta_r)h + w(D-h)(\theta_s-\theta_r)\{1+[\alpha(h-D)\cos i]^{n_1}\}^{(-1/n_1)} \end{aligned} \tag{6a}$$

The first and second terms on the right side of equation (6a) represent the total water content in saturated and unsaturated zone, respectively. The extents of saturated and unsaturated zones vary with the drainage process, leading to changes in the integral interval (i.e., from h to D) for the second term and subsequently in the calculated value of equation (6a). Figure 2a schematically shows the variation of the integral interval at different time moments (e.g., T1, T2, T3, T4, and T5). From T1 to T2, the thickness of the unsaturated zone increases as the water table declines; thus, the integral interval rises, representing more water content in the unsaturated zone. As the decline of the water table continues, h approaches 0 at time T3, and the integral interval equals the aquifer thickness (D); the corresponding water content in the unsaturated zone reaches its maximum value.

After time T3, the fully unsaturated zone begins to develop. As stated above, the absolute value of the negative pressure in the fully unsaturated zone increases with the further decline of the water table. Under such conditions, the integral interval remains unchanged (equals D) but shifts upward (see the range T3 → T4 → T5 in Figure 2a), resulting in a narrower integral area. At time T5, the integral area has declined sharply, indicating a marked reduction in the water content in the unsaturated zone. To describe the variations of the water content in the unsaturated zone, the following expression can be used:

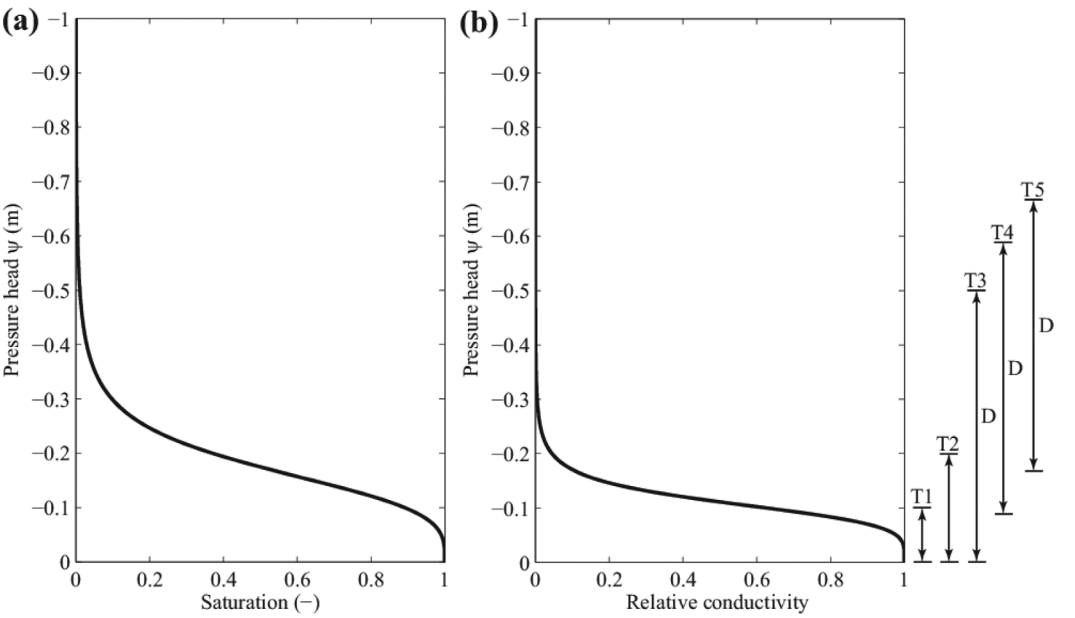

Figure 2. Schematic diagram of variations in the integral intervals for (a) water content in the unsaturated zone and (b) equivalent propagation thickness of the unsaturated flow at different moments.

$$S=w\int_0^D(\theta_s-\theta_r)\{1+[\alpha(h-z)\cos i]^{n_1}\}^{(-1-1/n_1)}\mathrm{d}z$$
$$=w(\theta_s-\theta_r)(D-h)\{1+[\alpha(h-D)\cos i]^{n_1}\}^{-1/n_1}+wh(\theta_s-\theta_r)[1+(\alpha h\cos i)^{n_1}]^{-1/n_1} \tag{6b}$$

Therefore,

$$\frac{\partial S}{\partial t}=\frac{\partial S}{\partial h}\frac{\partial h}{\partial t}=fw\frac{\partial h}{\partial t} \tag{7a}$$

$$f=(\theta_s-\theta_r)\left\{1-[1+(\alpha(h-D)\cos i)^{n_1}]^{-1-1/n_1}\right\},h\geq 0 \tag{7b}$$

$$f=(\theta_s-\theta_r)\left\{[1+(\alpha h\cos i)^{n_1}]^{-1-1/n_1}-[1+(\alpha(h-D)\cos i)^{n_1}]^{-1-1/n_1}\right\},h<0 \tag{7c}$$

Equations (7b) and (7c) can be unified as follows because they are continuous at $h=0$:

$$f=(\theta_s-\theta_r)\left\{[1+(\alpha\cdot\min(h,0)\cdot\cos i)^{n_1}]^{-1-1/n_1}-[1+(\alpha(h-D)\cos i)^{n_1}]^{-1-1/n_1}\right\} \tag{7d}$$

Comparison of the characteristic curves of saturation pressure and relative conductivity pressure based on equation (4a) shows that they have similar distribution features (Figure 3). To derive the analytical expression of the terms $\int_h^D K(\psi)\mathrm{d}z$ and $\int_0^D K(\psi)\mathrm{d}z$ in equation (3a), we transformed the hydraulic conductivity expression in equation (4a) and expressed it in a format similar to that used in equation (5):

$$K(\psi)=K_s\left[\frac{1}{1+(\beta\psi)^{n_2}}\right]^{(1+1/n_2)} \tag{8}$$

where β [L^{-1}] and n_2 are parameters related to the soil properties that determine the conductivity ($n_2\neq n_1$). To date, there are four parameters in the modified van Genuchten functions, which can be determined by fitting the original van Genuchten functions (i.e., α, n_1, β, and n_2). To prove the rationale behind the modified van Genuchten functions, we compared the errors among characteristic curves plotted using equations (5) and (8) and the original van Genuchten functions of equation (4a) for four soil types: sand, clay, loam, and laboratory sand. The root-mean-square error (RMSE) of S_W and $K(\psi)/K_s$ were less than 1% and 2%, respectively, in all cases (Table 1). This suggests that the modified van Genuchten functions can

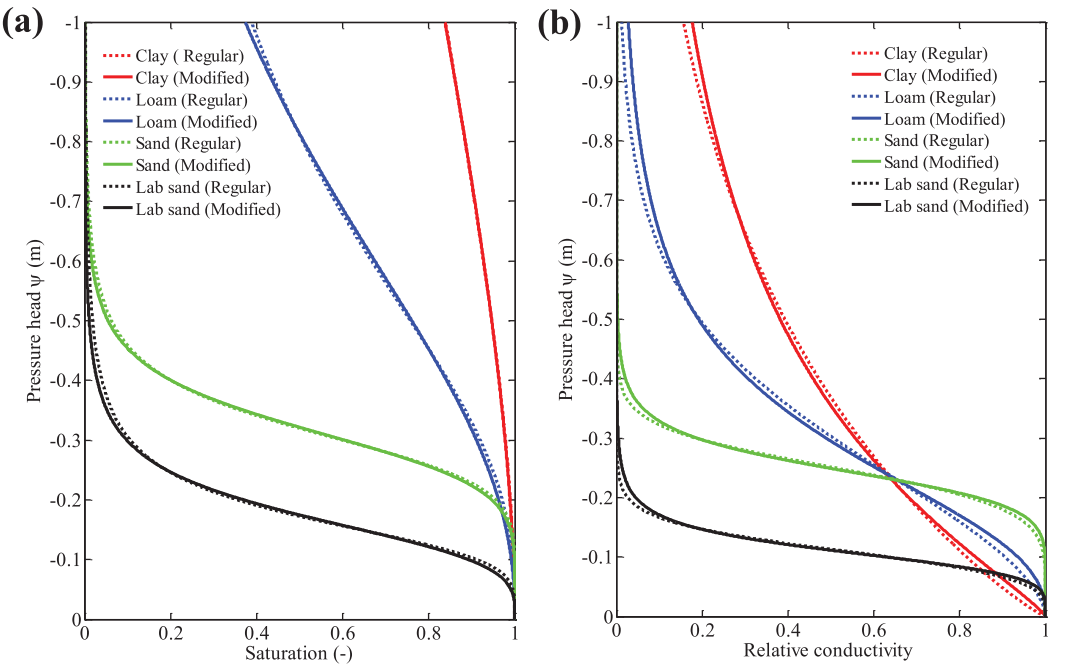

Figure 3. Comparison of the regular and modified van Genuchten functions of (a) saturation and (b) relative conductivity of different soil types.

accurately describe the soil characteristics described by the original van Genuchten function (Figure 3). Although the van Genuchten function has its own limitation to approximate the observed infiltrometer results [*Ippisch et al.*, 2006], the predicted saturation pressure and relative conductivity pressure tendency are suitable for most engineering practices. Limitation of the van Genuchten function for each type of sand was not observed in this study. Within the scope of effective application, the proposed modified van Genuchten function can be considered to be a feasible approximation. For the theoretical derivation, the modified van Genuchten function was used.

Similar to the integration of equation (6a), when $h \geq 0$ (early and middle drainage stages), integrating equation (8) with respect to z along the direction normal to the slope from the water table ($z=h$) to the surface ($z=D$) yields the following:

$$\int_h^D K(\psi)\mathrm{d}z = K_s(D-h)\{1+[\beta(h-D)\cos i]^{n_2}\}^{-1/n_2} \tag{9a}$$

The value of equation (9a) reaches a maximum at time T3 when $h = 0$. Since time T3, $h < 0$, and only the unsaturated zone exists. Integrating equation (8) with respect to z along the direction normal to the slope from the slope base ($z=0$) to the surface ($z=D$) yields the following:

Table 1. Regular and Modified van Genuchten Parameters for Sand, Loam, Clay, and Laboratory Sand [Hilberts et al., 2005]

Parameter	Sand	Loam	Clay	Laboratory Sand
Regular				
α_{VG}	−0.0324	−0.0161	−0.0066	−0.063
n	6.66	2.6632	1.8601	4.4545
Modified				
α	−0.03	−0.0099	−0.0029	−0.0524
n_1	5.9051	2.2264	1.7393	3.6499
β	−0.0393	−0.0279	−0.0146	−0.0849
n_2	7.4302	2.3691	1.1859	4.6721
RMSE (S_W)	0.52%	0.64%	0.06%	0.78%
RMSE ($K(\psi)/K_s$)	0.86%	1.65%	1.27%	0.74%

$$\begin{aligned}\int_0^D K(\psi)\mathrm{d}z = K_s(D-h)\\ \{1+[\beta(h-D)\cos i]^{n_2}\}^{-1/n_2}\\ +K_s h[1+(\beta h\cos i)^{n_2}]^{-1/n_2}\end{aligned} \tag{9b}$$

From time T3 to T5 (Figure 2b), the integral interval remains unchanged (D) but moves upward, leading to a smaller integral area. The value of equation (9b), therefore, decreases accordingly. Because equations (9a)

and (9b) are continuous at $h=0$, the unsaturated flux along the direction perpendicular to the hillslope can be expressed as:

$$q_{us}=-K_s\frac{\partial\Phi}{\partial x}\left\{(D-h)[1+(\beta(h-D)\cos i)^{n_2}]^{-1/n_2}+\min(h,0)\cdot[1+(\beta h\cos i)^{n_2}]^{-1/n_2}\right\} \quad (10)$$

By summing the flows in saturated and unsaturated zones, we derived the modified HSB model:

$$wf\frac{\partial h}{\partial t}=-\frac{\partial wq}{\partial x}+Nw \quad (11a)$$

$$q=-K_s[\max(h,0)+P]\left(\frac{\partial h}{\partial x}\cos i+\sin i\right) \quad (11b)$$

$$P=(D-h)[1+(\beta(h-D)\cos i)^{n_2}]^{-1/n_2}+\min(h,0)\cdot[1+(\beta h\cos i)^{n_2}]^{-1/n_2} \quad (11c)$$

The difference between the modified HSB model presented in this study and the revised HSB model of *Hilberts et al*. [2005] lies in the treatment of the drainage flux along the hillslope. Combined (i.e., saturated and unsaturated flow) and single (i.e., only unsaturated flow) drainage processes are both considered based on equation (11b). The additional flux term equation (11c) can be considered to represent the additional amount of drainage included apart from that in the saturated zone. This additional drainage occurs in the capillary fringe and the unsaturated zone. Therefore, we defined the term P as the equivalent propagation thickness, which is related to the slope angle, soil properties, pressure head, and aquifer thickness.

3. Model Validation

Because the analytical solution is difficult to determine directly, we used the finite difference method to discretize equation (11) for numerical values (see supporting information for details). We validated the proposed new HSB model against the numerical results simulated with SUTRA [*Voss and Provos*, 2008] and the experimental results of *Hilberts et al*. [2005]. In this study, we considered two types of hillslope configurations: convergent and divergent (Figure 4). Following the work of *Hilberts et al*. [2005], the aquifer thicknesses (D) of the convergent and divergent hillslope configurations were 0.48 and 0.44 m, respectively. The initial and boundary conditions of HSB model and SUTRA are both consistent with the experimental setup used by *Hilberts et al*. [2005]. The initial pore water pressure was set to be hydrostatic based on the initial water table height measured from the experiments. In terms of boundary conditions, the outlet was assigned a Dirichlet-type boundary condition with a pressure head of 0.05 m, and the other end of the hillslope was set to be no-flux.

The validation process involved two steps. In the first step, to demonstrate the effects of unsaturated flow on hillslope drainage, we used the simulated results from SUTRA to compare the proposed HSB model with previous models. In the second step, we further compared different HSB models in terms of accuracy using the experimental data.

3.1. Comparison With the SUTRA Model

We used the 3-D, variable-saturation, variable-density groundwater modeling code SUTRA [*Voss and Provos*, 2008], which is based on Richards' equation, to simulate the hillslope drainage processes (i.e., both convergent and divergent) with a slope of 10% for two soil types: lab sand ($Ks = 4.63 \times 10^{-4}$ m/s) and loam ($Ks = 2.89 \times 10^{-6}$ m/s). Additional parameters used in this model are listed in Table 1. The simulation results were then used to compare the proposed HSB model with other models. Tests on the dependency on mesh size and time step were conducted to ensure that the numerical results presented in this study are convergent.

Figures 5 and 6 compare the predicted variations of the water table and outflow rate for lab sand, respectively. In the supporting information, Figures S2 and S3 show the comparison results for the loam hillslope. The proposed HSB model yielded more accurate prediction than the previous HSB models, and such an improvement is more prevalent for loam soil. The improved accuracy is primarily produced by the proposed HSB model's consideration of the continuous drainage in the fully unsaturated zone of the late stage, which is neglected by the other models. The outflow rates predicted by the HSB model of *Hilberts et al*. [2005] are lower than those of the traditional HSB model (Figure 6 and Figure S3). Additionally, the water table predicted by Hilbert et al.'s model decreases faster than the traditional HSB model (Figure 5 and Figure S2); this

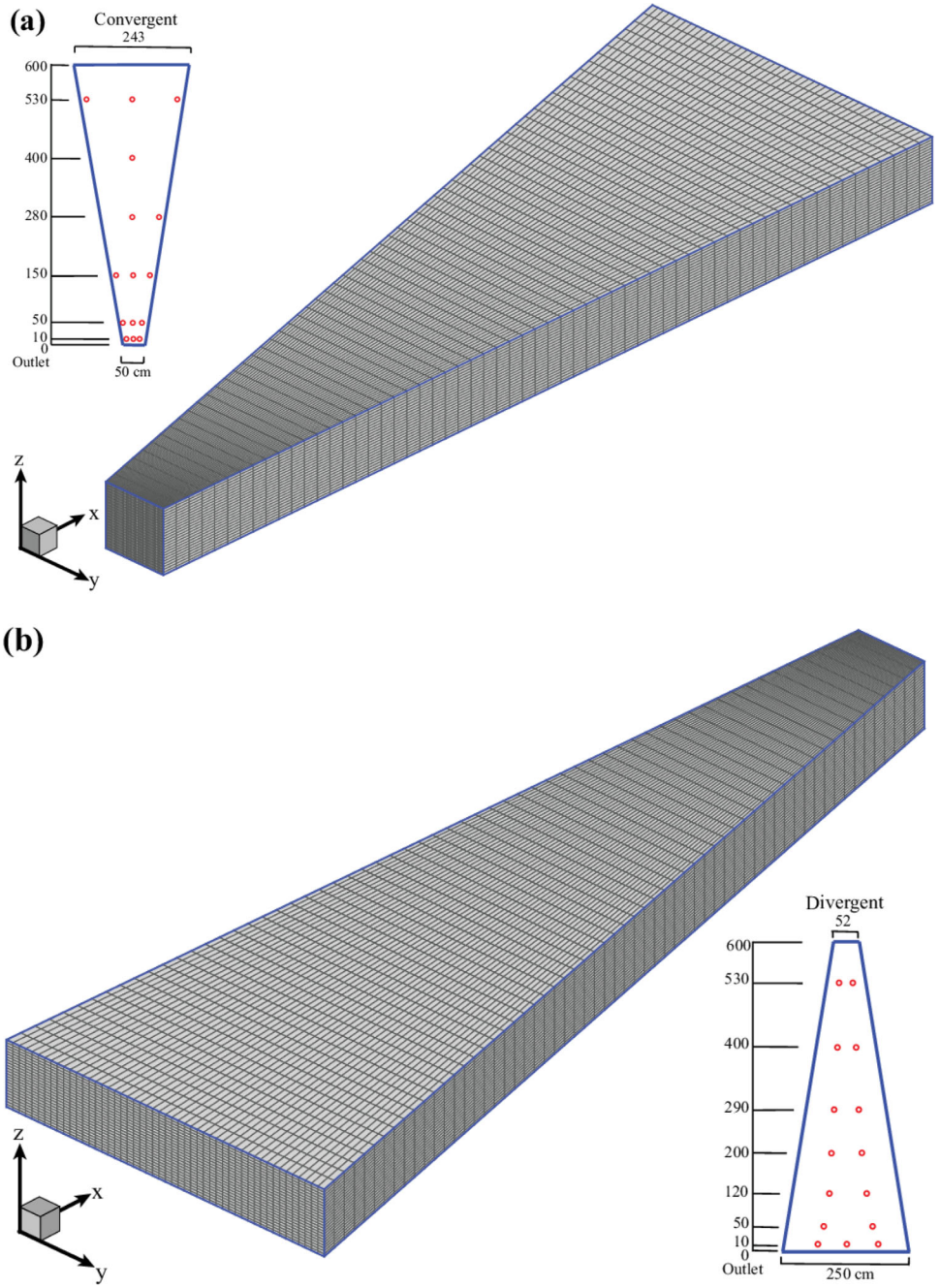

Figure 4. The 3-D view of (a) convergent and (b) divergent laboratory slopes with circles indicating the positions of piezometer [*Hilberts et al*., 2005].

is because the model of *Hilberts et al*. [2005] retains a certain amount of water in the unsaturated zone. In comparison, the predictions of the proposed HSB model are more similar to the simulation results.

More importantly, the traditional and Hilbert et al.'s HSB models only predict positive water tables because $q=q_s=0$ when $h=0$ in these models; this means that the water in the unsaturated zone is forced to remain stagnant and thus stops the drainage process. However, as discussed above, the negative pressure in the fully unsaturated zone varies in practice and redistributes the remaining pore water, a portion of which causes flow toward the outlet (Figure 1b). The proposed HSB model considers this feature and can thus predict the negative pressure variation in the fully unsaturated zone. The comparison shown in Figure 5 and Figure S2 shows that the negative pressure prediction using the proposed HSB model is similar to the

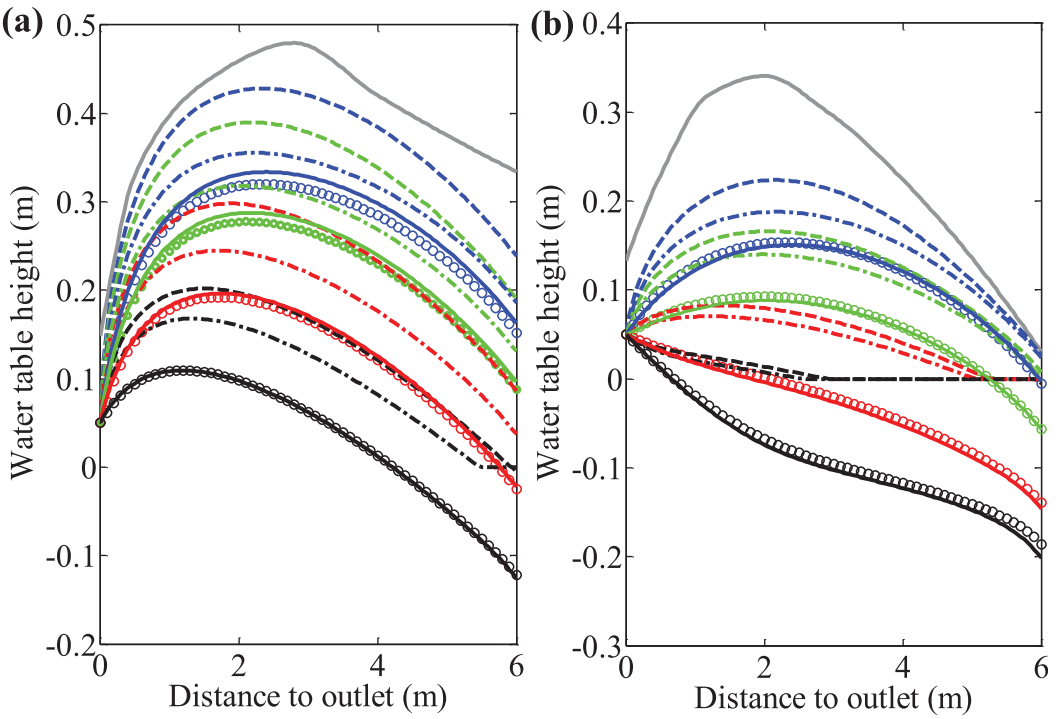

Figure 5. Water table profiles for (a) convergent and (b) divergent sand-composed hillslope configurations with a slope of 10% at the following times in hours: 0 (gray), 1 (blue), 2 (green), 5 (red), and 10 (black). Circles represent the simulated results produced by the SUTRA model; the dashed lines represent those of the original HSB model; the dash-dotted lines represent those of the revised HSB model of *Hilberts et al.* [2005]; the solid lines represent those of the proposed HSB model.

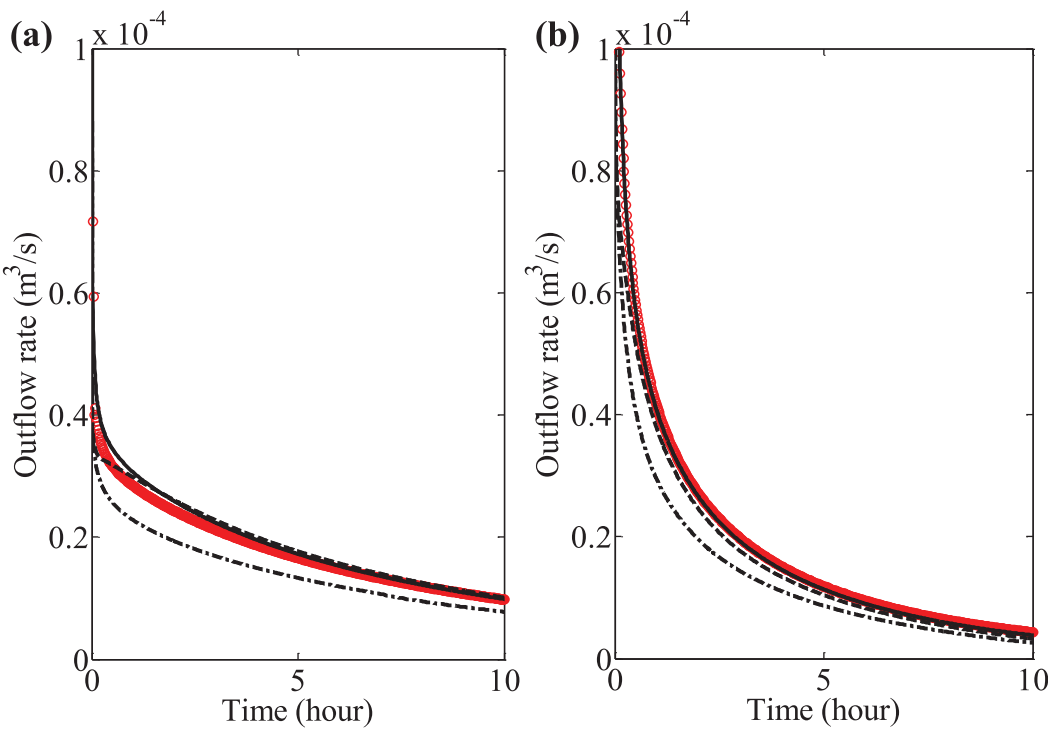

Figure 6. Outflow rates for (a) convergent and (b) divergent sand-composed hillslope configurations with a slope of 10%. Red circles represent the simulated results produced by SUTRA model; the dashed lines represent those of the original HSB model; the dash-dotted lines represent those of the revised HSB model of *Hilberts et al.* [2005]; the solid lines represent those of the proposed HSB model.

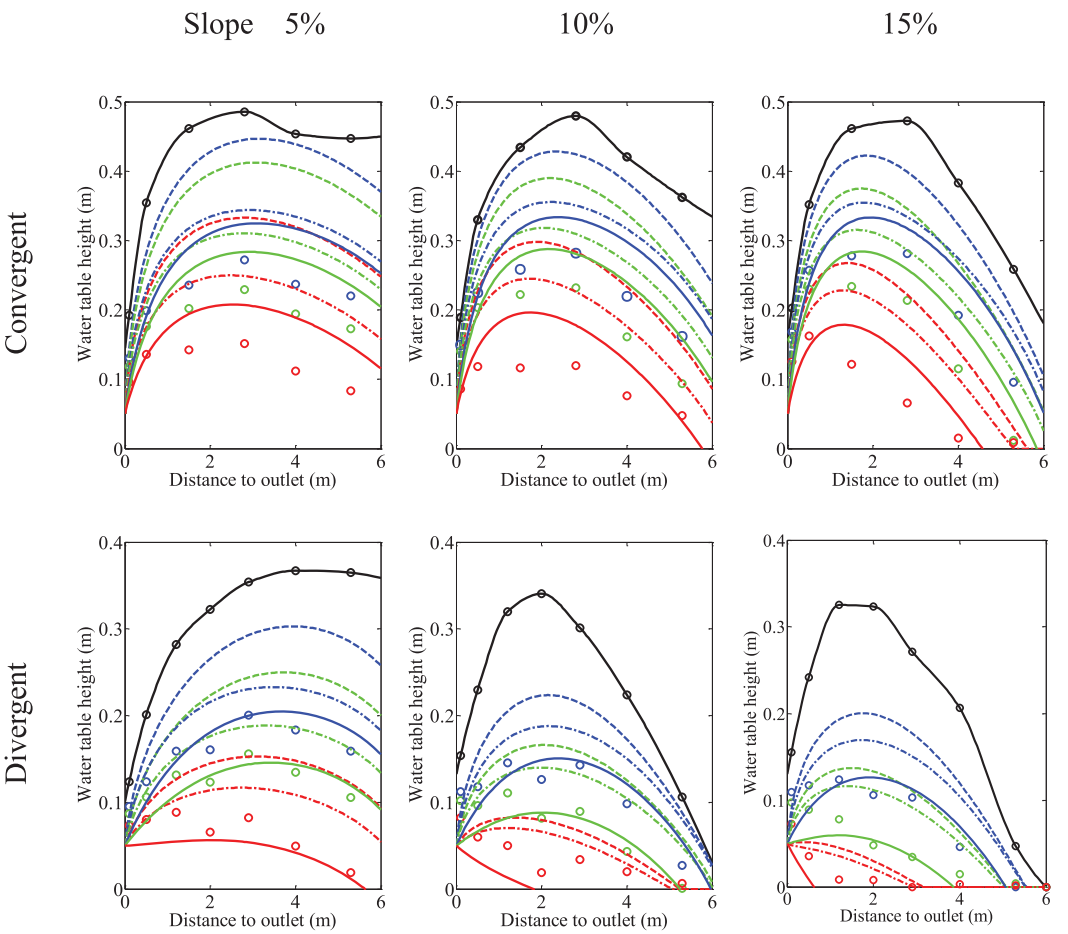

Figure 7. Water table profile for uncalibrated HSB models for six hillslope configurations at the following times in hours: 0 (black), 1 (blue), 2 (green), and 5 (red). Circles represent measured values; the dashed lines represent the original HSB model; the dash-dotted lines represent the revised HSB model of *Hilberts et al.* [2005]; the solid lines represent the proposed HSB model.

simulation results of SUTRA. It is shown that the variation of the negative pressure is nonlinear, particularly under the divergent configuration. The variation of the negative pressure head confirms the continuous unsaturated flow during the late drainage stage.

3.2. Comparison With Experimental Data

To further analyze the accuracy and applicability of the new HSB model, we compared it against other HSB models using experimental results. This study considered convergent and divergent hillslopes, with a total of six configurations: three slopes for each type of hillslope (e.g., 5%, 10%, and 15%). The hydraulic conductivity (K_s) was measured to be 40 m/d; the parameters of lab sand are listed in Table 1. Figure 7 compares the measured and predicted water table profiles using different HSB models based on uncalibrated parameters. When unsaturated flow along the hillslope is considered, the HSB model presented in this study was more precise at predicting the water table profile compared to other HSB models. The higher drainage at the outlet, which resulted from unsaturated flow, led to a faster decline in the water table. However, the corresponding accuracy of the prediction of the outflow rate was lower (Figure 8). Additionally, because unsaturated flow is considered, the proposed HSB model can better reproduce the feature of concavity during the middle and late stages of the divergent hillslope drainage process. However, in the absence of parameter calibration, the proposed model predicts an earlier occurrence of the end of the drainage process in the divergent configuration; therefore, the model should be further calibrated by reducing the conductivity K_s.

Following the method of *Hilberts et al.* [2005], which was based on the method of minimal prediction-error control for the outflow rate, we adjusted the permeability to increase the prediction accuracy; the adjusted permeability values for the proposed HSB model and the revised HSB model of *Hilberts et al.* [2005] are listed

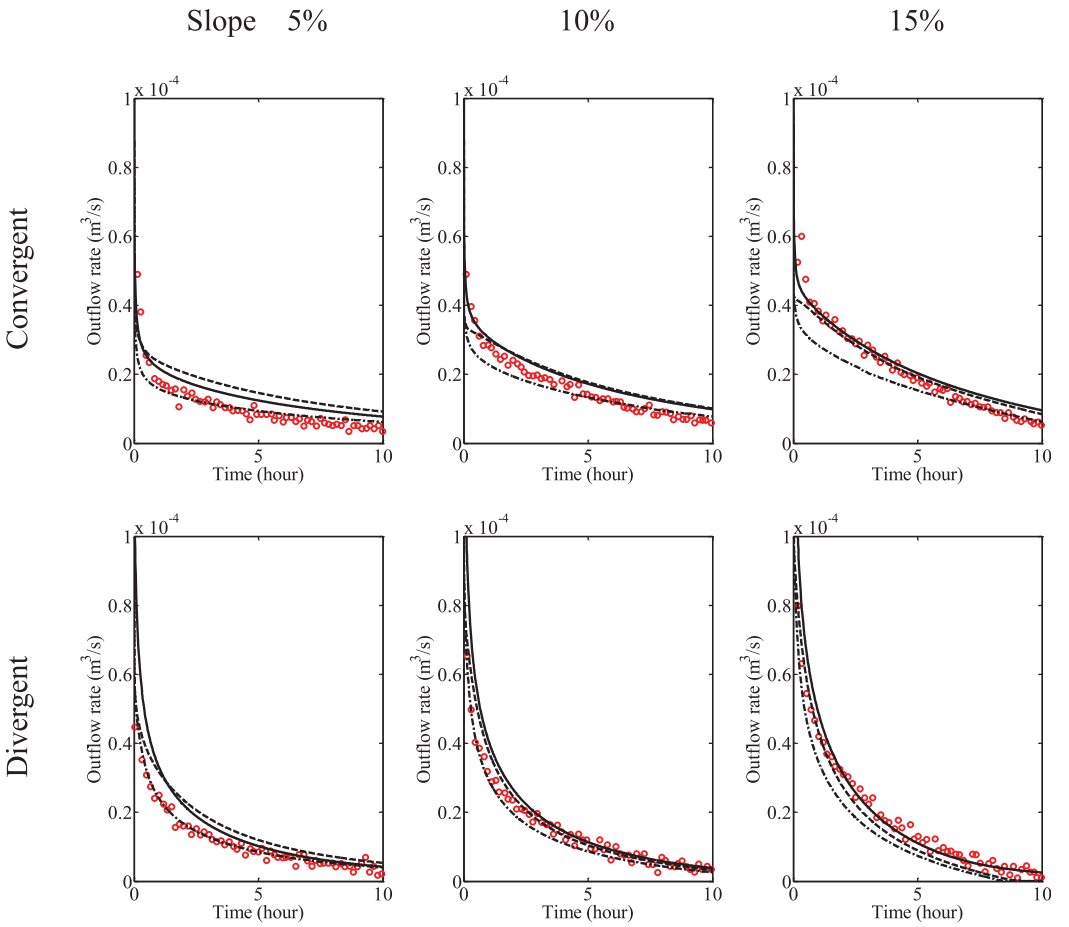

Figure 8. Outflow rates for uncalibrated HSB models for six hillslope configurations. Red circles represent measured values; the dashed lines represent the original HSB model; the dash-dotted lines represent the revised HSB model of *Hilberts et al.* [2005]; the solid lines represent the proposed HSB model.

in Table 2. The simulation results (Figures 9 and 10) indicate that when the accuracy requirement for water content prediction was satisfied, the two HSB models were similar in their predictions in the case of a convergent hillslope configuration. However, in the case of a divergent hillslope configuration, the water table profile predicted by the proposed HSB model was more accurate. In particular, the predicted water table profiles at the second and fifth hours were considerably closer to the measured values. To quantitatively compare the simulated and experimental values, we introduced the mismatch index [*Willmott*, 1981] as follows:

$$d = 1 - \frac{\sum_{j=1}^{n} [C(j) - E(j)]^2}{\sum_{j=1}^{n} [|C(j) - \bar{E}| + |E(j) - \bar{E}|]^2} \tag{12}$$

where $C(j)$ is the predicted results, $E(j)$ is the experiment value, $\bar{E}$ is the mean value of $E(j)$, $d=0$ indicates a complete mismatch, and $d=1$ indicates a complete agreement. Table 3 shows the calculated mismatch indexes of the outflow rate for convergent and divergent cases. The mismatch indexes between the

Table 2. Calibrated Conductivity Value K_s (m/d) for Hilbert's HSB Model [*Hilbert et al.*, 2005] and the Proposed Revised Model at Different Slopes

	HSB Model [*Hilbert et al.*, 2005]			Presented HSB Model		
	5%	10%	15%	5%	10%	15%
Convergent	44	48	56	39	39	44
Divergent	32	34	31	21	27	30

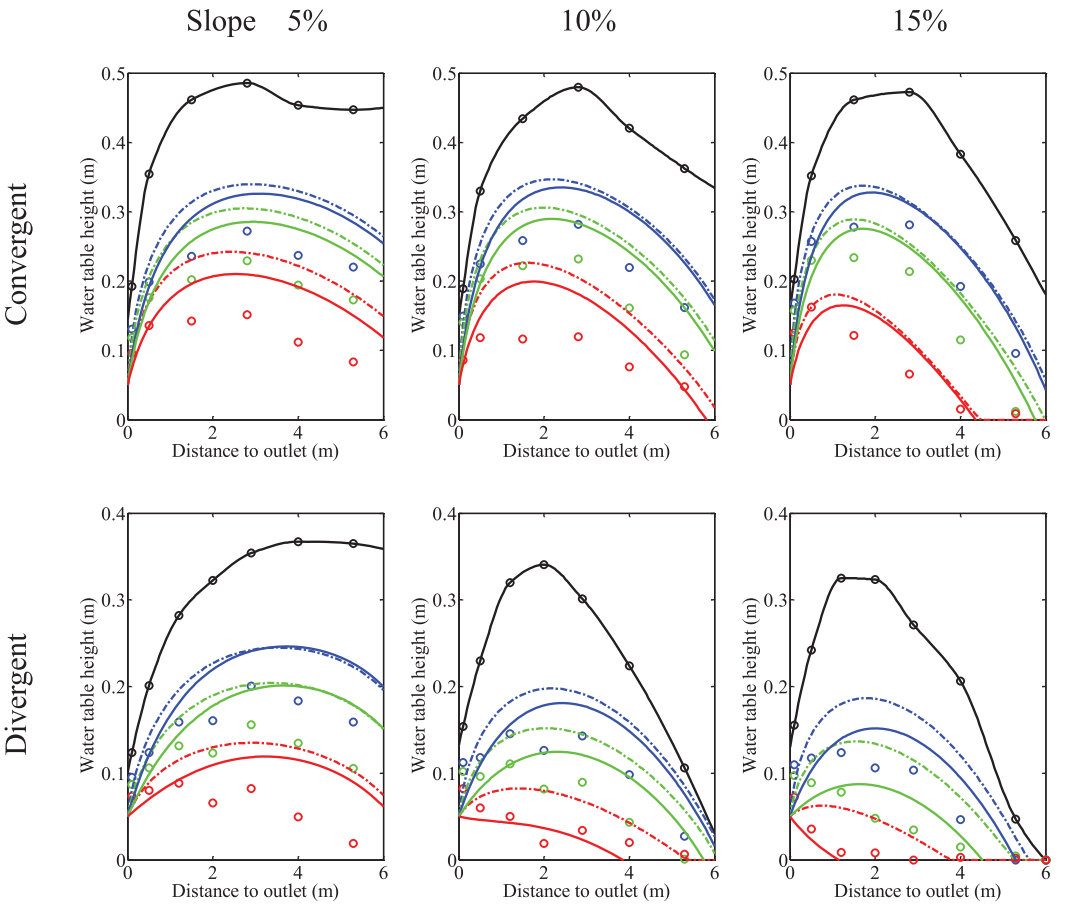

Figure 9. Water table profile for the calibrated HSB models for the six hillslope configurations. Profiles are shown for the following times in hours: 0 (black), 1 (blue), 2 (green), and 5 (red). Circles represent measured values; the dash-dotted lines represent the revised HSB model of *Hilberts et al*. [2005]; the solid lines represent the proposed HSB model.

traditional and proposed model are similar based on the minimal prediction-error control of the outflow rate. With respect to the time-dependent water table, we plotted the mismatch index versus time (Figure 11). Initially, $d=1$; however, as time progressed, the value of d changed due to the difference between the measured and predicted water level. A large discrepancy resulted in a lower value of d. A quantitative comparison showed an improvement with the proposed model when the index d was nearer to 1.

For drainage engineering, the time to drain and the depth of flow are two basic evaluation criteria [*Casagrande and Shannon*, 1952; *Moulton*, 1979]. For these two factors, the model presented in this study performed better at simulating the hillslope drainage process compared to the revised HSB model of *Hilberts et al*. [2005], particularly in the divergent hillslope configuration. This suggests that when the thickness of the unsaturated zone cannot be neglected, the effects of unsaturated flow on hillslope drainage are significant. However, although the new HSB model improves the prediction accuracy, the predicted values still deviate from the experimental results. The deviation might be because of the nonignorable dynamic pressure effect, which results from the vertical flow near the outlet, and the hysteresis effect in the unsaturated zone, which has been confirmed to play an important role in affecting groundwater flow [*Lehmann et al*., 1998; *Stauffer and Kinzelbach*, 2001; *Cartwright*, 2014].

4. Discussions

4.1. Rationale for Considering Unsaturated Lateral Flow

In this study, the derivation of an analytical solution assumes that the unsaturated zone experiences moisture flux along the hillslope and that it is necessary to consider this flux to improve the prediction accuracy

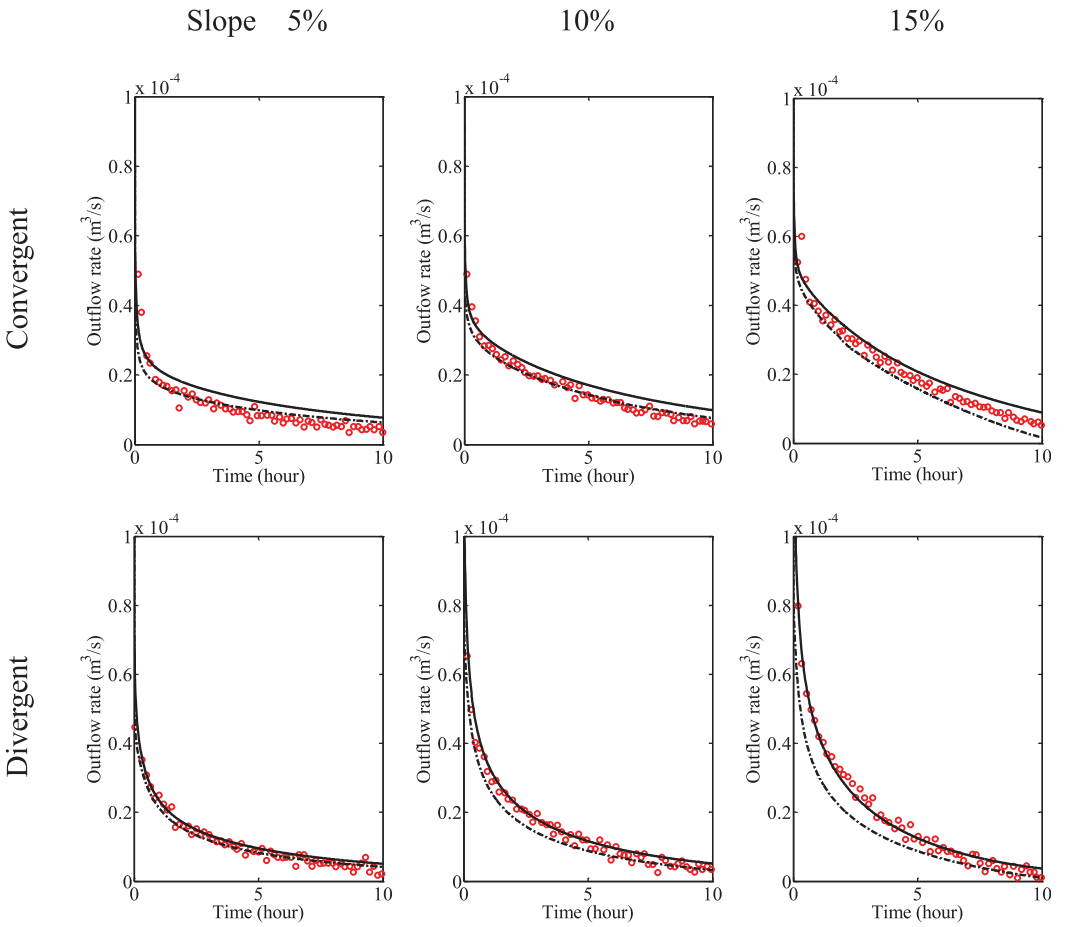

Figure 10. Outflow rates for the calibrated HSB models for the six hillslope configurations. Red circles represent measured values; the dash-dotted lines represent the revised HSB model proposed of *Hilberts et al.* [2005]; the solid lines represent the proposed HSB model.

of the HSB model. However, this assumption needs to be tested. To address this concern, we used SUTRA [*Voss and Provos*, 2008] to simulate the velocity field (i.e., both convergent and divergent) with a slope of 10% for two soil types (i.e., lab sand and loam). Figures 12 and 13 show the simulated flow field and water table at the first, second, and fifth hours for the convergent and divergent sand hillslopes; the simulated flow fields of the convergent and divergent loam hillslope configurations are shown in Figures S4 and S5 in the supporting information, respectively.

During drainage, the unsaturated and saturated flow directions are generally parallel to the base slope. The assumption of a hydrostatic pressure distribution along the direction normal to the hillslope was proved feasible in both the saturated zone and unsaturated zones. Although the unsaturated flow velocity is low, the nonnegligible drainage flux significantly influenced the spatial and temporal variations of the water table during drainage. Such flow features highlight the fact that it is necessary to consider unsaturated lateral flow in the HSB model. Based on the flow pattern shown, the unsaturated flow along the base slope shows that the horizontal and vertical flow components coexist. Thus, it is insufficient to depict the hillslope

Table 3. Mismatch Index With the Outflow Rate for Hilbert's HSB Model [*Hilbert et al.*, 2005] and the Proposed Revised Model at Different Slopes

	HSB Model [*Hilbert et al.*, 2005]			Present HSB Model		
	5%	10%	15%	5%	10%	15%
Convergent	0.912	0.984	0.985	0.910	0.962	0.985
Divergent	0.990	0.985	0.951	0.981	0.992	0.996

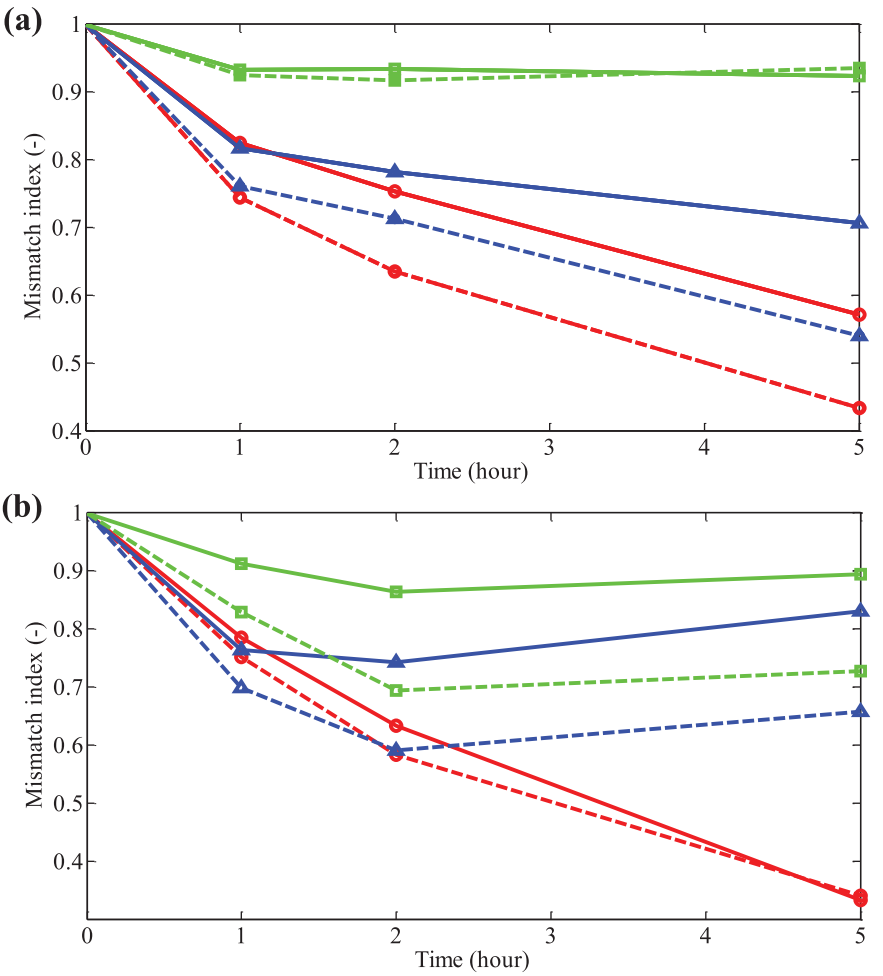

Figure 11. Variation of the mismatch index for (a) convergent and (b) divergent hillslope configurations. Dashed lines represent the revised HSB model of *Hilberts et al.* [2005], and solid lines represent the HSB model proposed in this study. The colors red, blue, and green represent the slopes of 5%, 10%, and 15%, respectively.

drainage by only coupling the traditional HSB model with the 1-D Richards' equation to consider the vertical flow in the unsaturated zone.

4.2. Variation of Drainable Porosity With Time

We compared the variations in the drainable porosity with time for different configurations along the slope base. These variations can be divided into two stages: in the early and middle drainage stages, both unsaturated and saturated zones exist, and the drainable porosity gradually approaches the effective porosity $(\theta_s - \theta_r)$ as the drainage process progresses (Figure 14). By considering unsaturated flow in the model, the rate calculated by this method was higher due to the more rapid decrease in the water table. When the water content in the surface of unsaturated zone approached θ_r, the decline of the water table no longer altered the water content in the upper saturated zone, leading to a linear relationship between the water content and the water table variation; the drainable porosity also reaches its maximum value at this time. In the late stage, when only the unsaturated zone exists above the hillslope base (Figure 1b), the drainable porosity began to decrease. Figure 2 shows that although the integral interval, which is equal to D, does not change, it moves upward and decreases the value calculated from equation (6). As a result, the ratio of the water content to the water table variation decreases, and the drainable porosity in the fully unsaturated zone continuous to decrease.

As shown by the variation of the drainable porosity, there is a shift from combined drainage (i.e., both the saturated and unsaturated zones exist) toward single drainage (i.e., only the unsaturated zone exists) above

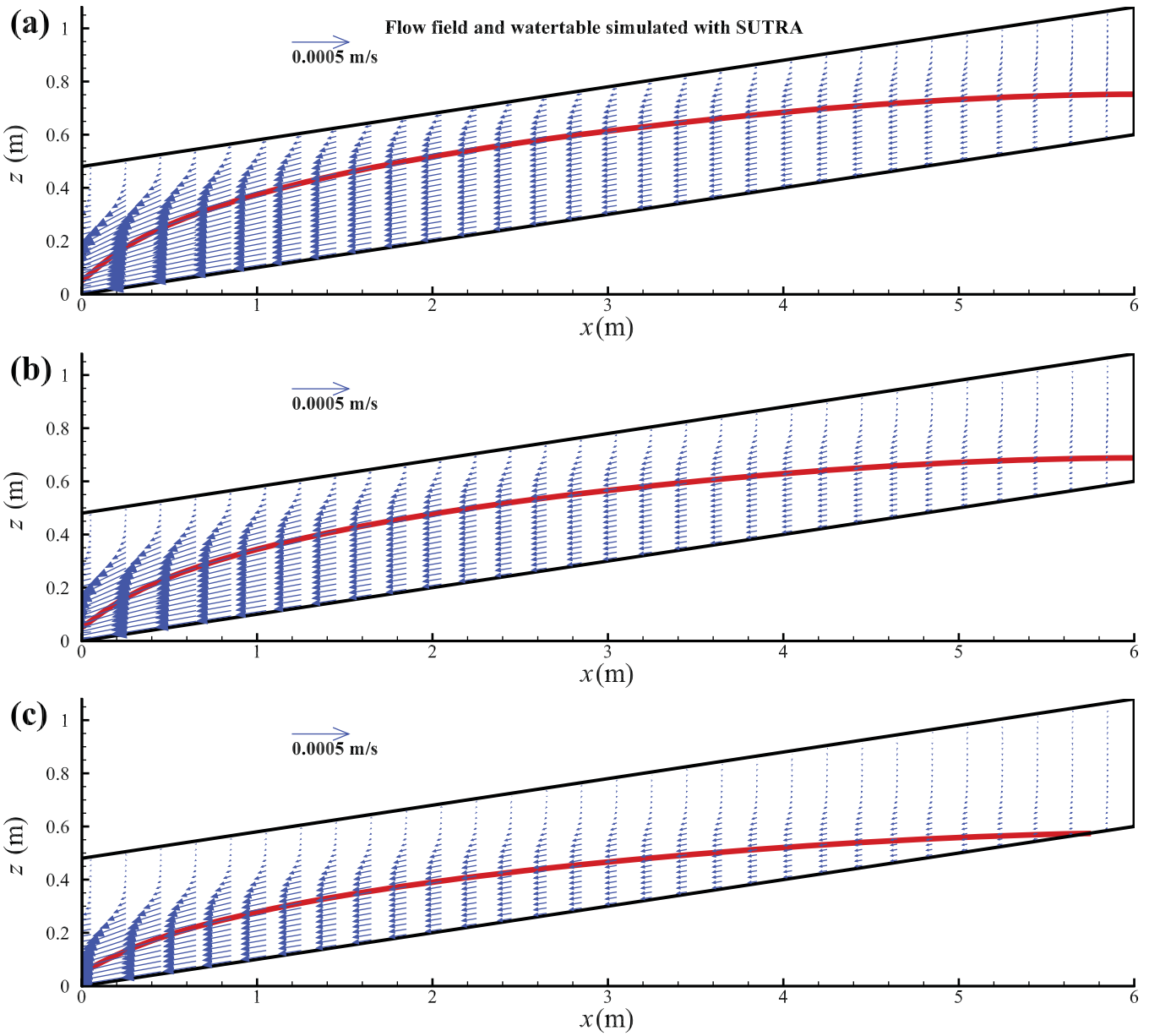

Figure 12. Flow field (blue arrows) and water table (red line) along a symmetric vertical cross section at the (a) first hour, (b) second hour, (c) fifth hour of the drainage process for a sand-composed convergent hillslope configuration with a 10% slope. The red solid line represents the water table above which the unsaturated zone exists.

the hillslope base; the drainable porosity is also shown to increase initially and then decrease. In comparison, a decrease in the water table was more rapid for a divergent hillslope configuration when unsaturated flow was considered, allowing the drainable porosity to vary more quickly.

4.3. Variation of the Equivalent Propagation Thickness

Based on equation (11c), we analyzed the effects of the unsaturated zone's thickness on the equivalent propagation thickness by considering three typical soil types: sand, loam, and clay. As shown in Figure 1a, when the saturated zone is below the unsaturated zone ($h > 0$), the equivalent propagation thickness at one fixed position tends to increase in tandem with the thickness of the unsaturated zone (Figure 15); this trend was most prominent in clay soils. As shown in Figure 2b, when the thickness of the unsaturated zone above the saturated zone is sufficiently large, the calculated value of equation (11c) approaches its maximum value. For example, when the thickness of the unsaturated zone reached 1 m (e.g., in the material example of *Hilberts et al.* [2005] with a slope of 10%), the equivalent propagation thicknesses P for sand,

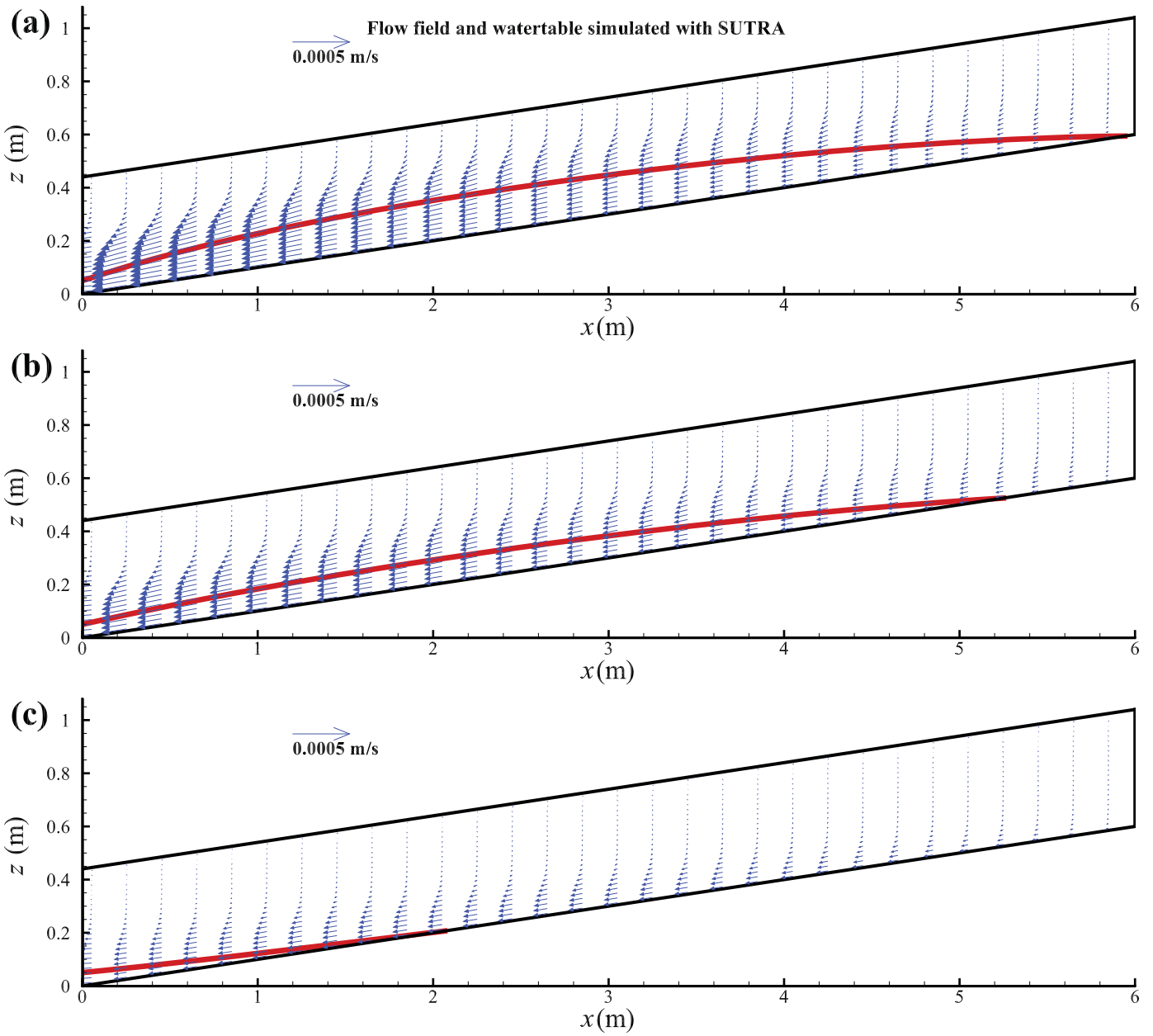

Figure 13. Flow field (blue arrows) and water table (red line) along a symmetric vertical cross section at the (a) first hour, (b) second hour, (c) fifth hour of the drainage process for a sand-composed divergent hillslope configuration with a 10% slope. The red solid line represents the water table above which the unsaturated zone exists.

loam, clay, and laboratory sand were 0.256, 0.348, 0.453, and 0.118 m, respectively. The value of P increased with increasing slope angle under the Dupuit assumption; these values have exceeded the thickness of the capillary fringe ψ_c [L]. *Vachaud and Vauclin* [1975] suggested incorporating the capillary fringe as an integral part of the Boussinesq aquifer by substituting h with $h+\psi_c$ to improve the simulated water table. Thus, the proposed HSB model showed that a correction of only the capillary fringe parameter would still underestimate the water outflow rate.

In the late drainage stage, the drainage in the fully unsaturated zone continues as the negative pressure changes when the fully unsaturated zone exists above the hillslope base, thereby replenishing the adjacent downslope zone. The equivalent propagation thickness is also related to the negative pressure: a higher absolute negative pressure yields a smaller equivalent propagation thickness. Figure 2b shows that, from time T3, the integral interval is equal to the aquifer thickness D. At time T4, the integral interval remains

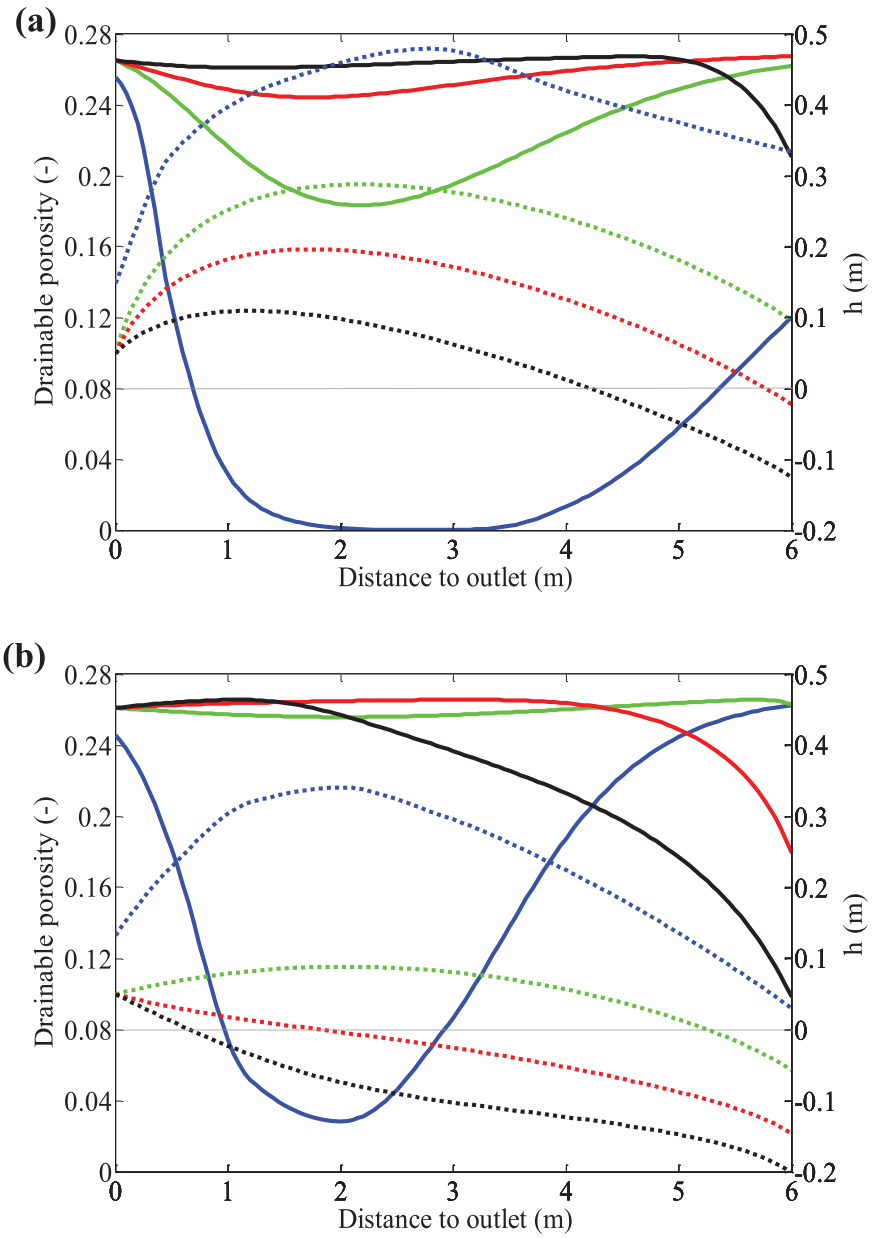

Figure 14. Drainage porosity profiles for (a) convergent and (b) divergent hillslope configurations during the drainage process at time (in hours): 0 (blue), 2 (green), 5 (red), and 10 (black). The solid line represents the drainage porosity, and each colored-dotted line represents the water table.

unchanged but shifts upward and the result of equation (11c) decreases and approaches zero. Figure 16 clearly shows that the equivalent propagation thickness in the unsaturated zone increases initially and then decreases. This trend first appears at the upstream hillslope during the stage in which only the unsaturated zone exists. Similar to the variation in the drainable porosity along the hillslope, the equivalent propagation thickness during the stage increases initially and then decreases. In comparison, for a divergent hillslope configuration, the decrease in the water table is more rapid, which allows the equivalent propagation thickness to change more quickly.

5. Concluding Remarks

By modifying the *van Genuchten* [1980] functions under the Dupuit and homogeneity assumptions, we proposed the concept of equivalent propagation thickness and derived its analytical expression. Two stages of

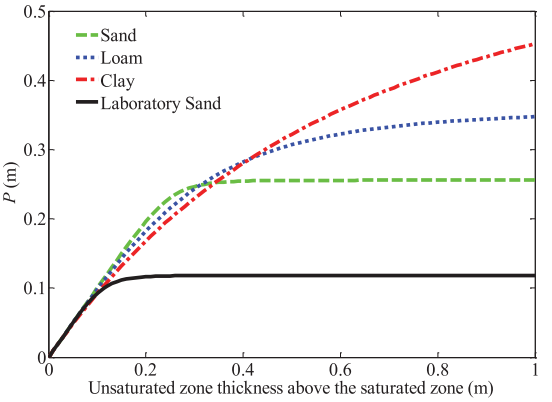

Figure 15. Equivalent propagation thicknesses in the vadose zone for different soil types when the unsaturated zone exists above the saturated zone.

drainage process were distinguished and introduced into the HSB model, which was initially proposed by *Troch et al.* [2003]. The main conclusions of this study are as follows:

1. The entire drainage process can be divided into two stages: (1) the early and middle saturated and unsaturated drainage stages and (2) the late unsaturated drainage stage. In the second stage, the flow in the unsaturated zone plays a major role. The hillslope drainage process in the late stage is primarily contributed by the drainage from the unsaturated zone as a result of the remaining pore water redistribution.
2. When the thickness of the unsaturated zone is not negligible, considering the unsaturated flow will markedly improve the prediction accuracy of the HSB model. This improvement was more apparent during the middle and late stages of the hillslope drainage process, when the unsaturated zone thickness was comparable to the saturated zone.
3. Along the hillslope, the drainable porosity and equivalent propagation thickness increase during the early and middle combined drainage processes and then decrease during the late unsaturated drainage process. This trend is more significant with divergent hillslope drainage processes because the thickness of the saturated zone decreases more rapidly.
4. The new HSB model can simulate the variation in the negative pressure head in the unsaturated zone, making it possible to future analyze the moisture variation in the unsaturated zone during the hillslope drainage process, which cannot be realized by previous HSB models.

Although present study reveals the effects of unsaturated flow on hillslope drainage, more research is needed to further advance our understanding of the process. As mentioned above, the dynamic pressure effect at the outlet and hysteresis effect in the unsaturated zone should be considered to improve the prediction accuracy. Besides, this study assumes the soils to be homogeneous whereas most hillslope aquifers are heterogeneous [*Rupp and Selker*, 2006]. Further theoretical studies should consider these factors to gain a deeper insight into the hillslope drainage process by combining specific experimental and numerical simulation work [*Hazenberg et al.*, 2015].

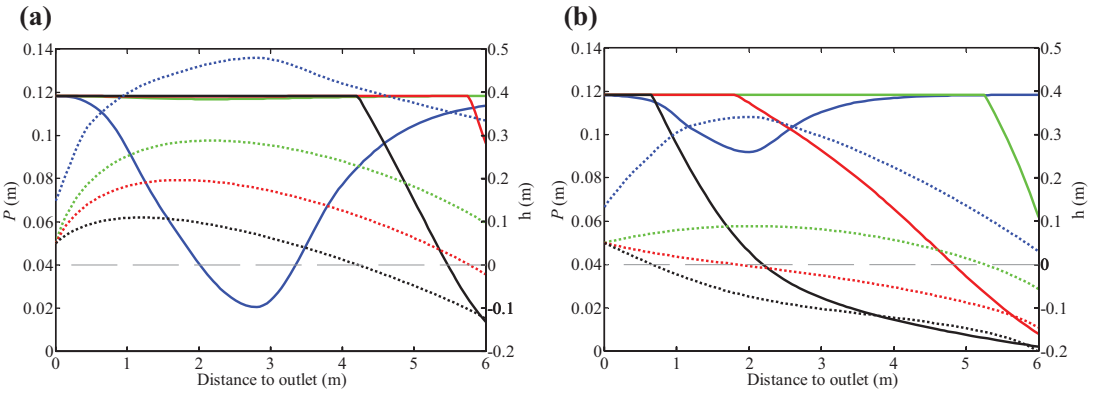

Figure 16. Equivalent propagation thicknesses (*P*) profiles for (a) convergent and (b) divergent sand-composed hillslope configurations during the drainage process at the following times in hours: 0 (blue), 2 (green), 5 (red), and 10 (black). The solid line represents the equivalent propagation thicknesses *P*, and each colored-dotted line represents the water table.

Acknowledgments
This study was supported by the National Basic Research Program of China (973 program, 2012CB417005), the National Natural Science Foundation of China (51479055), and the Fundamental Research Funds for the Central Universities (2015B15614 and 2015B25614). Data presented in the paper can be obtained through an e-mail request to the corresponding author. The authors would like to thank the Hydrology and Quantitative Water Management Group of Wageningen University for providing the experimental data analyzed in this study. Additionally, the authors would like to acknowledge the valuable comments from the reviewers, which led to significant improvement of this paper.

References

Barry, D. A., S. J. Barry, and J. Y. Parlange (1996), Capillarity correction to periodic solutions of the shallow flow approximation, in *Mixing in Estuaries and Coastal Seas*, edited by C. Pattiaratchi, pp. 496–510, AGU, Washington, D. C.

Bear, J. (1972), *Dynamic of Fluids in Porous Media*, Elsevier, N. Y.

Bresciani, E., P. Davy, and J. R. de Dreuzy (2014), Is the Dupuit assumption suitable for predicting the groundwater seepage area in hillslopes?, *Water Resour. Res.*, *50*, 2394–2406, doi:10.1002/2013WR014284.

Brutsaert, W. (1994), The unit response of groundwater outflow from a hillslope, *Water Resour. Res.*, *30*(10), 2759–2763, doi:10.1029/94WR01396.

Cardenas, M. B. (2010), Lessons from and assessment of Boussinesq aquifer modeling of a large fluvial island in a dam-regulated river, *Adv. Water Resour.*, *33*(11), 1359–1366, doi:10.1016/j.advwatres.2010.03.015.

Cartwright, N. (2014), Moisture-pressure dynamics above an oscillating water table, *J. Hydrol.*, *512*, 442–446, doi:10.1016/j.jhydrol.2014.03.024.

Cartwright, N., P. Nielsen, and P. Perrochet (2005), Influence of capillarity on a simple harmonic oscillating water table: Sand column experiments and modeling, *Water Resour. Res.*, *41*, W08416, doi:10.1029/2005WR004023.

Casagrande, A., and W. Shannon (1952), Base course drainage for airport pavements, *Trans. Am. Soc. Civ. Eng.*, *117*, 792–820.

Dahl, M., B. Nilsson, J. H. Langhoff, and J. C. Refsgaard (2007), Review of classification systems and new multi-scale typology of groundwater-surface water interaction, *J. Hydrol.*, *344*(1-2), 1–16, doi:10.1016/j.jhydrol.2007.06.027.

Dan, H. C., P. Xin, L. Li, and D. Lockington (2012), Boussinesq equation-based model for flow in the drainage layer of highway with capillarity correction, *J. Irrig. Drain. Eng.*, *138*(4), 336–348, doi:10.1061/(ASCE)IR.1943-4774.0000404.

Dan, H. C., P. Xin, L. Li, and L. Li (2013), Improved Boussinesq equation–based model for transient flow in a drainage layer of highway: Capillary correction, *J. Irrig. Drain. Eng.*, *139*(12), 1018–1027, doi:10.1061/(ASCE)IR.1943-4774.0000642.

Fink, J. P., J. Y. Parlange, and A. I. El-Kadi (2001), One last visit to the capillarity correction for free surface flow, *Water Resour. Res.*, *37*(3), 827–829, doi:10.1029/2000WR900318.

Gillham, R. W. (1984), The capillary fringe and its effect on water-table response, *J. Hydrol.*, *67*(1–4), 307–324, doi:10.1016/0022-1694(84)90248-8.

Hazenberg, P., Y. Fang, P. Broxton, D. Gochis, G. Y. Niu, J. D. Pelletier, P. A. Troch, and X. Zeng (2015), A hybrid-3D hillslope hydrological model for use in Earth system models, *Water Resour. Res.*, *51*, 8218–8239, doi:10.1002/2014WR016842.

Hilberts, A. G. J., P. A. Troch, and C. Paniconi (2005), Storage-dependent drainable porosity for complex hillslopes, *Water Resour. Res.*, *41*, W06001, doi:10.1029/2004WR003725.

Hilberts, A. G. J., P. A. Troch, C. Paniconi, and J. Boll (2007), Low-dimensional modeling of hillslope subsurface flow: Relationship between rainfall, recharge, and unsaturated storage dynamics, *Water Resour. Res.*, *43*, W03445, doi:10.1029/2006WR004964.

Hogarth, W. L., L. Li, D. A. Lockington, F. Stagnitti, M. B. Parlange, D. A. Barry, T. S. Steenhuis, and J. Y. Parlange (2014), Analytical approximation for the recession of a sloping aquifer, *Water Resour. Res.*, *50*, 8564–8570, doi:10.1002/2014WR016084.

Ippisch, O., H. J. Vogel, and P. Bastian (2006), Validity limits for the van Genuchten-Mualem model and implications for parameter estimation and numerical simulation, *Adv. Water Resour.*, *29*(12), 1780–1789, doi:10.1016/j.advwatres.2005.12.011.

Kong, J., C. J. Shen, P. Xin, Z. Y. Song, L. Li, D. A. Barry, D. S. Jeng, F. Stagnitti, D. A. Lockington, and J. Y. Parlange (2013), Capillary effect on water table fluctuations in unconfined aquifers, *Water Resour. Res.*, *49*, 3064–3069, doi:10.1002/wrcr.20237.

Kong, J., P. Xin, G. F. Hua, Z. Y. Luo, C. J. Shen, D. Chen, and L. Li (2015), Effects of vadose zone on groundwater table fluctuations in unconfined aquifers, *J. Hydrol.*, *528*, 397–407, doi:10.1016/j.jhydrol.2015.06.045.

Lehmann, P., F. Stauffer, C. Hinz, O. Dury, and H. Flühler (1998), Effect of hysteresis on water flow in a sand column with a fluctuating capillary fringe, *J. Contam. Hydrol.*, *33*(1–2), 81–100, doi:10.1016/S0169-7722(98)00066-7.

Moench, A. F. (2008), Analytical and numerical analyses of an unconfined aquifer test considering unsaturated zone characteristics, *Water Resour. Res.*, *44*, W06409, doi:10.1029/2006WR005736.

Moulton, L. (1979), *Groundwater, Seepage, and Drainage: A Textbook on Groundwater and Seepage Theory and Its Application*, U.S. Dep. of Transp., Fed. Highway Admin., Washington, D. C.

Nachabe, M. H. (2002), Analytical expressions for transient specific yield and shallow water table drainage, *Water Resour. Res.*, *38*(10), 1193, doi:10.1029/2001WR001071.

Neuman, S. P. (1987), On methods of determining specific yield, *Ground Water*, *25*(6), 679–684, doi:10.1111/j.1745-6584.1987.tb02208.x.

Paniconi, C., P. A. Troch, E. E. van Loon, and A. G. J. Hilberts (2003), Hillslope-storage Boussinesq model for subsurface flow and variable source areas along complex hillslopes: 2. Intercomparison with a three-dimensional Richards equation model, *Water Resour. Res.*, *39*(11), 1317, doi:10.1029/2002WR001730.

Parlange, J. Y., and W. Brutsaert (1987), A capillarity correction for free surface flow of groundwater, *Water Resour. Res.*, *23*(5), 805–808, doi:10.1029/WR023i005p00805.

Phi, S., W. Clarke, and L. Li (2013), Laboratory and numerical investigations of hillslope soil saturation development and runoff generation over rainfall events, *J. Hydrol.*, *493*, 1–15, doi:10.1016/j.jhydrol.2013.04.009.

Rocha, D., J. Feyen, and A. Dassargues (2007), Comparative analysis between analytical approximations and numerical solutions describing recession flow in unconfined hillslope aquifers, *Hydrogeol. J.*, *15*(6), 1077–1091, doi:10.1007/s10040-007-0170-4.

Romano, C. G., E. O. Frind, and D. L. Rudolph (1999), Significance of unsaturated flow and seepage faces in the simulation of steady-state subsurface flow, *Ground Water*, *37*(4), 625–632, doi:10.1111/j.1745-6584.1999.tb01151.x.

Rupp, D. E., and J. S. Selker (2006), On the use of the Boussinesq equation for interpreting recession hydrographs from sloping aquifers, *Water Resour. Res.*, *42*, W12421, doi:10.1029/2006WR005080.

Serrano, S. E. (1995), Analytical solutions of the nonlinear groundwater flow equation in unconfined aquifers and the effect of heterogeneity, *Water Resour. Res.*, *31*(11), 2733–2742, doi:10.1029/95WR02038.

Stauffer, F., and W. Kinzelbach (2001), Cyclic hysteretic flow in porous medium column: Model, experiment, and simulations, *J. Hydrol.*, *240*(3–4), 264–275, doi:10.1016/S0022-1694(00)00382-6.

Troch, P. (1993), Conceptual basin-scale runoff process models for humid catchments: Analysis, synthesis and applications, PhD thesis, 247 pp., Ghent Univ., Ghent, Netherlands.

Troch, P., E. van Loon, and A. Hilberts (2002), Analytical solutions to a hillslope-storage kinematic wave equation for subsurface flow, *Adv. Water Resour.*, *25*(6), 637–649, doi:10.1016/S0309-1708(02)00017-9.

Troch, P. A., C. Paniconi, and E. E. van Loon (2003), Hillslope-storage Boussinesq model for subsurface flow and variable source areas along complex hillslopes: 1. Formulation and characteristic response, *Water Resour. Res.*, *39*(11), 1316, doi:10.1029/2002WR001728.

Troch, P. A., A. H. van Loon, and A. G. J. Hilberts (2004), Analytical solution of the linearized hillslope-storage Boussinesq equation for exponential hillslope width functions, *Water Resour. Res.*, *40*, W08601, doi:10.1029/2003WR002850.

Troch, P. A., et al. (2013), The importance of hydraulic groundwater theory in catchment hydrology: The legacy of Wilfried Brutsaert and Jean-Yves Parlange, *Water Resour. Res.*, *49*, 5099–5116, doi:10.1002/wrcr.20407.

Vachaud, G., and M. Vauclin (1975), Comment on "A numerical model based on coupled one-dimensional Richards and Boussinesq equations" by Mary F. Pikul, Robert L. Street, and Irwin Remson, *Water Resour. Res.*, *11*, 506–509, doi:10.1029/WR011i003p00506.

van Genuchten, M. T. (1980), A closed-form equation for predicting the hydraulic conductivity of unsaturated soils, *Soil Sci. Soc. Am. J.*, *44*(5), 892–898, doi:10.2136/sssaj1980.03615995004400050002x.

Verhoest, N. E. C., and P. A. Troch (2000), Some analytical solutions of the linearized Boussinesq equation with recharge for a sloping aquifer, *Water Resour. Res.*, *36*, 793–800, doi:10.1029/1999WR900317.

Voss, C. I., and A. M. Provos (2008), SUTRA: A model for saturated-unsaturated, variable-density ground-water flow with solute or energy transport, U.S. Geol. Surv. Water Resour. Invest. Rep., *02-4231*, 291 p.

Willmott, C. J. (1981), On the validation of models, *Phys. Geogr.*, *2*(2), 184–194, doi:10.1080/02723646.1981.10642213.